

## Reversible Binding of Nitric Oxide and Carbon–Carbon Bond Formation in a Meso-hydroxylated Heme

Sankar Prasad Rath, Richard Koerner,<sup>†</sup> Marilyn M. Olmstead, and Alan L. Balch\*

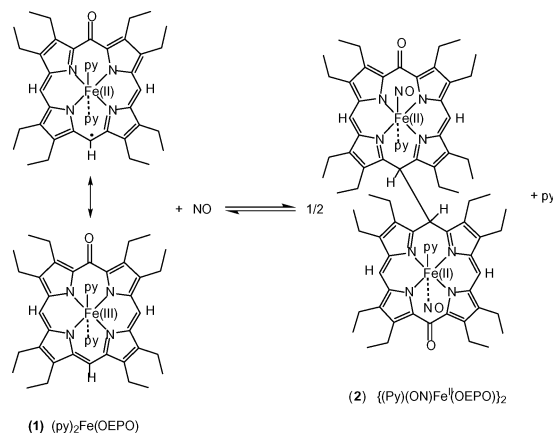
Department of Chemistry, University of California, Davis, One Shields Avenue, Davis, California 95616

Received March 6, 2003; E-mail: albalch@ucdavis.edu

Heme oxygenase (HO), which converts heme as a substrate into biliverdin,<sup>1</sup> and coupled oxidation, treatment of heme with dioxygen in the presence of a reducing agent,<sup>2</sup> involve introduction of meso hydroxy group in the initial stage of heme cleavage. However, the details of the next stages of heme oxidation have received little study. The model complex (py)<sub>2</sub>Fe(OEPO) (**1**) (OEPO is the trianion of octaethylxorphlorin, py is pyridine) is a stable intermediate which has been isolated and characterized crystallographically<sup>3</sup> and spectroscopically,<sup>4</sup> but which also reacts readily with dioxygen to undergo ring opening to eventually produce biliverdin.<sup>2</sup> Unfortunately, the reaction of **1** with dioxygen occurs without the buildup of detectable concentrations of observable intermediates.<sup>2</sup> To explore the reactivity of **1** further, we have examined its ability to interact with nitric oxide, a small molecule known to bind to hemes in a fashion similar to that of dioxygen.<sup>5</sup>

Exposure of a 3 mM pyridine solution of **1** at 22 °C to nitric oxide under the strict exclusion of dioxygen results in a color change from green to red-brown and the formation of a new species {(py)(ON)Fe(OEPO)}<sub>2</sub> (**2**) as shown in Scheme 1. The reaction

### Scheme 1



has been monitored by <sup>1</sup>H NMR spectroscopy as shown in Figure 1. Trace A shows a portion of the <sup>1</sup>H NMR spectrum of **1** which has been reported previously.<sup>4</sup> Trace B shows the spectrum of the same sample after the addition of nitric oxide. All of the resonances of **1** have disappeared, and a new set of resonances due to **2** has grown. Purging the solution with dinitrogen reverses the reaction. Trace C shows the same sample after a short purge with dinitrogen. The resonances of **2** have diminished in intensity, while those of **1** have grown. Further purging with dinitrogen results in the loss of all resonances of **2**. The resulting solution can then be treated with nitric oxide to reform the resonances of **2**.

For clarity, only a portion of the paramagnetically shifted <sup>1</sup>H NMR spectrum of **2** is shown in Figure 1 which exhibits meso

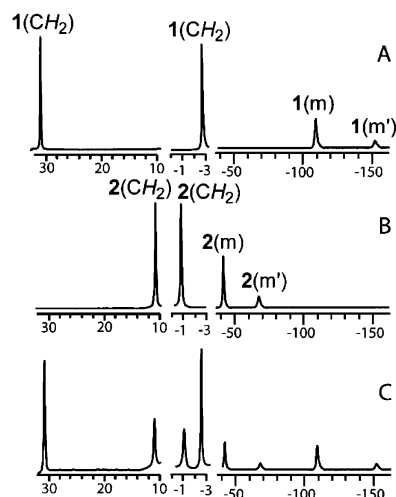


**Figure 1.** <sup>1</sup>H NMR spectra (400 MHz) of a solution of (py)<sub>2</sub>Fe(OEPO) (A) before addition of NO, (B) after exposure to NO, and (C) after partial purging with N<sub>2</sub>. All spectra were taken at 22 °C in the strict absence of O<sub>2</sub>. Resonances labeled **1** are assigned to (py)<sub>2</sub>Fe(OEPO) **1**, while those labeled **2** are assigned to {(py)(ON)Fe(OEPO)}<sub>2</sub> (**2**). Resonances from the meso protons are labeled m and m', while those of the methylene groups are labeled CH<sub>2</sub>.

resonances at −67.4 and −42.1 ppm and methylene resonances at −0.9 and 10.9 ppm at 22 °C. At −10 °C where all of the resonances are well resolved, the entire <sup>1</sup>H NMR spectrum of **2** consists of eight equally intense methylene resonances with chemical shifts of 18.9, 8.4, 4.3, 2.0, 1.6, 1.2, −1.6, −4.8 ppm, two meso resonances at −95.9 and −148.2 ppm, and four methyl resonances at 2.4, 1.8, 1.4, 1.2 ppm. This pattern of resonances indicates that the two sides of the porphyrin are different in the product and is consistent with the structure obtained from crystallography.

Careful layering of a dioxygen-free, nitric oxide-saturated *n*-hexane solution over the solution of **2** in pyridine resulted in the gradual crystallization of black plates of **2**·py in 50% yield. The structure of these crystals has been determined by X-ray crystallography.<sup>6</sup> Figure 2 shows a view of the entire molecule. The asymmetric unit consists of a (py)(ON)Fe(OEPO) portion which is connected to a second portion through a new C–C bond. There is a crystallographic center of symmetry at the middle of this bond. The C15–C15A bond distance (1.610(5) Å) is long but comparable to the corresponding distance (1.614(8) Å) in the related dimer {Ni<sup>II</sup>-(OEPO)}<sub>2</sub>.<sup>7</sup> The Fe–N–O unit is ordered and directed toward the meso-O=C function of the macrocycle and away from the C15–C15A bond that joins the two porphyrins. The macrocyclic ligand has a ruffled distortion that places C5 and C15 on the same side of the porphyrin as the Fe–NO group and positions the C5–O1 group with its short C=O bond distance (1.237(3) Å) in close proximity to the NO ligand. Since further attack upon **1** by O<sub>2</sub> involves reaction in the vicinity of the oxygenated meso position, the

<sup>†</sup> Deceased, December 17, 2002.

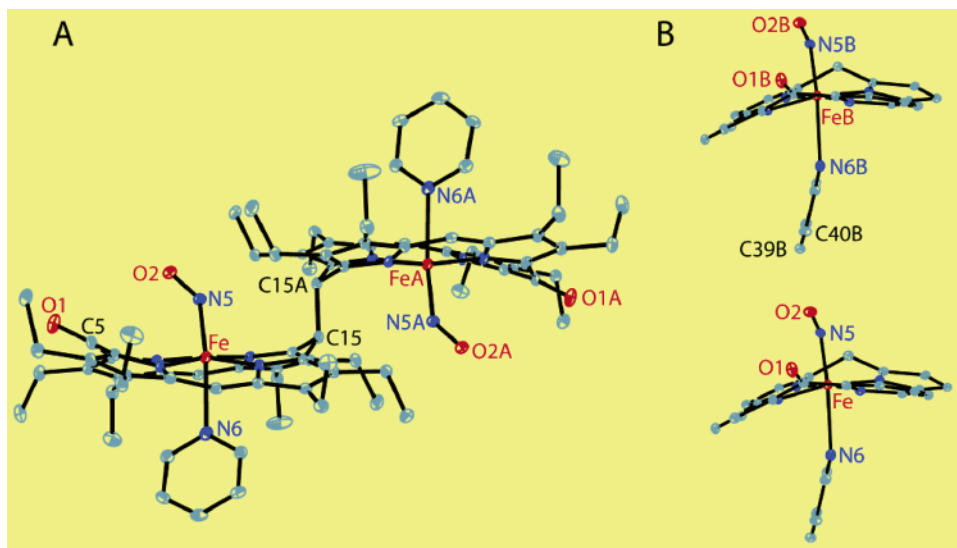


**Figure 2.** (A) Perspective view of  $\{(\text{py})(\text{ON})\text{Fe}(\text{OEPO})\}_2$  showing 30% thermal contours for all non-hydrogen atoms. Selected bond distances (Å): Fe–N1, 1.978(2); Fe–N2, 1.983(2); Fe–N3, 2.012(2); Fe–N4, 2.009(2); Fe–N5, 1.744(2); Fe–N6, 2.310(2); N5–O2, 1.190(3); O1–C5, 1.237(3); C15–C15', 1.610(5). Selected bond angles (deg): O2–N5–Fe, 138.3(2); N5–Fe–N1, 91.27(10); N5–Fe–N2, 89.88(10); N5–Fe–N3, 98.63(10); N5–Fe–N4, 97.31(10); N5–Fe–N6, 173.19(10); N6–Fe–N1, 81.98(9); N6–Fe–N2, 89.05(9); N6–Fe–N3, 88.11(9); N6–Fe–N4, 83.83(9); N1–Fe–N3, 170.09(9); N2–Fe–N4, 172.81(9). (B) Drawing of two half-molecules of  $\{(\text{py})(\text{ON})\text{Fe}(\text{OEPO})\}_2$  (ethyl groups omitted) which emphasizes the tilting of the axial pyridine ligands and shows the interaction between the NO group of one molecule with the pyridine ligand of another. The nonbonded O2...C40B and O2...C39B distances are 3.429(3) and 3.625(4) Å.

positioning of the NO ligand so that the O2...C5 distance is only 3.100(3) Å presents a highly suggestive model for the next stage of attack upon the heme periphery.

The dimensions of the Fe–N–O portion are similar to those found in five- and six-coordinate hemes of other  $\{\text{FeNO}\}^7$  units.<sup>8,9</sup> The Fe–N–O unit is bent at an angle of 138.3(2)°, and the Fe–N5 bond is short 1.744(2) Å. The N5–O2 bond is unusually long, 1.190(3) Å, for an ordered NO.<sup>8</sup> The Fe–N5 bond is tilted by 5.2° from perpendicular to the plane of the N<sub>4</sub> unit, and the iron is asymmetrically positioned with two short (1.978(2), 1.983(2) Å) and two longer (2.009(2), 2.012(2) Å) Fe–N(pyrrole) distances. These features are similar to those in (ON)Fe(OEP).<sup>10</sup> The Fe–N6 distance (2.310(2) Å) is much longer, as are other Fe–N distances to axial ligands in six-coordinate  $\{\text{FeNO}\}^7$  hemes.<sup>8</sup> The infrared spectrum of the solid shows  $\nu(\text{NO})$  at 1645 cm<sup>-1</sup>.

As seen in B of Figure 2, the pyridine ligand is tilted away from the N5–Fe–N6 axis. This distortion appears to be a result of the molecular packing that places the NO group of an adjacent molecule near the pyridine ligand, but an electronic effect such as that observed for (ON)Fe(OEP)(*p*-C<sub>6</sub>H<sub>4</sub>F)<sup>11</sup> may be operative.

The formation of the dimer **2** can be viewed as a coupling of two ligand radicals that results from stabilization of the upper resonance structure of **1** in Scheme 1 by coordination of NO to the Fe(II) form of this complex. Reactions with NO should be informative in examining the reactivity of meso-oxygenated hemes that are protected from dimerization through incorporation of suitable substituents or in proteins such as HO.

**Acknowledgment.** We thank the NIH (Grant GM-26226) for support and the NSF for partial funding of NMR (OSTI 97-24412) and X-ray diffraction (CHE-9808259) instrumentation.

**Supporting Information Available:** X-ray crystallographic data for **2** in CIF format. This material is available free of charge via the Internet at <http://pubs.acs.org>.

## References

- (1) (a) Maines, M. D. *Heme Oxygenase: Clinical Applications and Functions*; CRC Press: Boca Raton, FL, 1992. (b) Ortiz de Montellano, P. R. *Acc. Chem. Res.* **1998**, *31*, 543.
- (2) St Claire, T. N.; Balch, A. L. *Inorg. Chem.* **1999**, *38*, 684. Balch, A. L.; Latos-Grażyński, L.; Noll, B. C.; Olmstead, M. M.; Sztrenberg, L.; Safari, N. *J. Am. Chem. Soc.* **1993**, *115*, 1422.
- (3) Balch, A. L.; Koerner, R. J.; Latos-Grażyński, L.; Noll, B. C. *J. Am. Chem. Soc.* **1996**, *118*, 2760.
- (4) Morishima, I.; Shiro, Y.; Wakino, T. *J. Am. Chem. Soc.* **1985**, *107*, 1063. Morishima, I.; Shiro, Y.; Hiroshi, F. *Inorg. Chem.* **1995**, *34*, 1528. Kalish, H. R.; Latos-Grażyński, L.; Balch, A. L. *J. Am. Chem. Soc.* **2000**, *122*, 12478. Balch, A. L. *Coord. Chem. Rev.* **2000**, *200–202*, 349.
- (5) Moller, J. K. S.; Skibsted, L. H. *Chem. Rev.* **2002**, *102*, 1167. Ford, P. C.; Lorkovic, I. M. *Chem. Rev.* **2002**, *102*, 993. Cheng, L.; Richter-Addo, G. B. In *The Porphyrin Handbook*; Kadish, K. M., Smith, K. M., Guillard, R., Eds.; Academic Press: New York, 2000; Vol. 4, p 219.
- (6) Crystal data for C<sub>87</sub>H<sub>101</sub>Fe<sub>2</sub>N<sub>13</sub>O<sub>4</sub>: black plate, triclinic, space group *P*-1, *a* = 10.582(2) Å, *b* = 13.246(3) Å, *c* = 14.854(3) Å,  $\alpha$  = 102.930(4)°,  $\beta$  = 96.721(7)°,  $\gamma$  = 102.373(11)°, *V* = 1952.2(7) Å<sup>3</sup>, *Z* = 1, *D*<sub>c</sub> = 1.280 Mg/m<sup>3</sup>, *T* = 90(2) K.; *R*1 = 0.116, *wR*2 = 0.135 for all data; conventional *R*1 = 0.055 computed for 5682 observed data (*I* > 2 $\sigma$ (*I*)) with 0 restraints and 471 parameters.
- (7) Balch, A. L.; Noll, B. C.; Reid, S. M.; Zovinka, E. P. *J. Am. Chem. Soc.* **1993**, *115*, 2531.
- (8) Scheidt, W. R.; Ellison, M. K. *Acc. Chem. Res.* **1999**, *32*, 350. Wyllie, G. A.; Scheidt, W. R. *Chem. Rev.* **2002**, *102*, 1067.
- (9) For the  $\{\text{FeNO}\}^n$  nomenclature see: Enemark, J. H.; Feltham, R. D. *Coord. Chem. Rev.* **1974**, *13*, 339.
- (10) Ellison, M. K.; Scheidt, W. R. *J. Am. Chem. Soc.* **1997**, *119*, 7404.
- (11) Richter-Addo, G. B.; Wheeler, R. A.; Hixson, C. A.; Chen, L.; Khan, M. A.; Ellison, M. K.; Schulz, C. A.; Scheidt, W. R. *J. Am. Chem. Soc.* **2001**, *123*, 6314.

JA035032B